New Stator Tooth for Reducing Torque Ripple in Outer Rotor Permanent Magnet Machine

Yusuf OZOGLU
Istanbul University, 34850, Istanbul, Turkey
yozoglu@istanbul.edu.tr

***Abstract*—Torque ripple has been a major problem for the permanent magnet (PM) machine. It is discussed focusing on the magnetic circuit of the PM machine. Since it is known the relationship between the torque ripple and the magnetic energy that is stored in the magnetic field along the air gap of the PM machine, fluctuation in the magnetic energy was initially revealed. New tooth geometry was obtained by drilling holes into stator tooth to modify this variation in the magnetic energy and the fluctuation in torque. Thus, a new stator tooth design in outer rotor surface-mounted permanent magnet (OR-SPM) machine was proposed to minimizing the torque ripple in this study. Improvement in torque ripple value was performed in excess of 50% thanks to new stator tooth design. In addition, improvements have been carried out at the average torque and total harmonic distortions (THD) of back EMF (electromotive force).**

***Index Terms*—stator, torque, minimization, finite element analysis, permanent magnet machine.**

I. INTRODUCTION

Permanent Magnet Synchronous Machines PMSMs have high efficiency and high torque density, high winding factor and relative small copper loss. PMSMs with concentrated fractional-pitch stator windings are increasingly used because of their lower copper loss. However, SPM machines have high torque ripple, cogging torque and large unbalanced magnetic forces.

It is shown that the vibration source is cogging torque of the radius direction in compliance with a magnetic energy from between stator and the rotor. The notch is established in the rotor because notch could be applied most easily to interior PM (IPM) motor and maximizes a reduction effect of cogging torque [1]. Three types of rotor surfaces, such as conventional round, slightly cut, and smoothed cut shape are studied. It is shown that the sinusoidal distribution of the air gap flux density has taken an effect on the reduction torque ripple of IPMSM [2]. The partly enlarged air gap length made by unequal rotor out diameter and stator core cutting is introduced in interior permanent magnet brushless DC motor (IPM BLDC). Adding holes in rotor core is used for good solution that both the cogging torque and the torque ripple reduction is extremely low [3].

The torque ripple is reduced by shifting the pole pairs by half a slot pitch and choosing the appropriate magnet width of PM motors [4]. It is shown that the segmentation of the arced magnet pole with radial magnetization into several arced magnet blocks with radial magnetization per pole can lead to a significant reduction of the cogging torque. An analytic formulation using Fourier coefficients of the square of the air-gap flux density function is proposed to determine the optimal configurations [5]. Both the lower original and newly introduced harmonics of cogging torque to reduce the cogging torque by PM shifting are investigated. The analytical expression of cogging torque with asymmetry magnet is obtained [6]. Study shows that the torque ripple can either decrease or increase after magnet skewing when step-skew techniques are used. Torque ripple reduction using skewing is more effective in machines that have a higher optimum skew angle. However, torque ripple in some motors will increase even after magnet skew, if the magnet shape is not designed carefully [7]. An analytical method based on the Maxwell equations to minimize torque ripple in the PMSM with bread-shape PM is proposed. The magnet pole shape is optimized by using this analytical method [8]. The effectiveness of skewing on torque ripple reduction of PM machines has been investigated with/without magnet shaping under different loadings and skewing angles. The effectiveness of skewing largely depends on the axial variation of the torque ripple phase but less on its magnitude under skewing is found [9]. The rotor pole shaping along with the pole shifting is analyzed. Magnet shifting is utilized for the torque improvement and shaping of the rotor pole outer surface is done to reduce the cogging torque of IPM BLDC motor [10].

The influence of the pole/slot combinations on cogging torque for motors with a number of slots per pole per phase is investigated. It is shown that skewing the stator slot opening would distribute the effects of interaction of the PM edge and slot opening during a rotation of a slot pitch [11]. The design tradeoff between the open-circuit cogging torque and the on-load torque ripple by taking the design of slot opening as an example. It is shown that the on-load cogging increases significantly, especially when a small slot opening width is adopted, which is opposite to the condition for minimizing the open-circuit cogging torque [12]. The influence of the slot opening on the cogging torque is investigated. It is shown that the cogging torque in PM and BLDC motors, where the number of magnet poles is close to the number of armature slots, can be reduced considerably by adjusting the width of the slots [13]. Two methods to reduce cogging torque, both based on the analysis of the rotational symmetry in a BLPM motor is studied. The first one uses asymmetrical distribution of the magnets on the rotor. The other uses the auxiliary slots method. Both cogging reduction methods reduce significantly the cogging torque [14]. It is shown that the slot/pole combination has a great effect on the cogging torque, and influences the optimal value of both skew angle and magnet arc, as well as determining the optimal number of auxiliary teeth/slots [15].

Digital Object Identifier 10.4316/AECE.2016.03008

The various techniques, including introducing in the stator teeth a number of notches, have been presented. Simple and effective model of the cogging torque mechanism has been introduced, which allows an easy explanation of the different strategies [16]. It is shown that the auxiliary slots are put on the pole face of the magnetizing yoke, which results in a not fully magnetized zone at the PM. Through Fourier expansion of the field and armature functions, the position and shape of the not fully magnetized zone that eliminate the cogging torque are found [17].

The cogging torque reduction in PM motors has been studied by varying the geometry shape of saliencies of the armature core on stator. Reduction mechanism is explained by the minimum net integral of product of normal and tangential magnetic flux with respect to the mechanical angle [18]. Optimum design of armature pole shape is carried out using design sensitivity analysis and evolution strategy whose design variables are based on the harmonic balance method for BLDC motors [19]. New air gap profile is defined by a dip and a dip angle for single-phase PM BLDC motor to improve starting torque and to reduce cogging torque. Various air gap profiles can be generated and profiles with dip angle less than critical dip angle improves the starting torque compared to existing air gap profiles [20]. It is found that the 6^{th} torque ripple harmonic is partially produced by non-symmetrical peak flux density distributions in the stator teeth, due to interaction of the permanent magnet flux with armature flux in tooth-coil winding (TCW) PMSM. It is shown that the 6^{th} harmonic can be eliminated by teeth widths adjustment, whereas conventional skewing technique is not appropriate for the reduction of this harmonic [21].

The above studies can be classified according to part of the machine that is studied to modify for reducing the torque ripple and/or the cogging torque. They focus on the rotor core [1, 2], both the rotor and stator core [3], the magnet [4-9] both the rotor core and magnet [10], the slot [11, 12], both the slot and magnet [13-17], and the tooth [18-21].

It will be focused exclusively on the tooth and partially on the slot opening to overcome the torque ripple in this study. However, it will be also studied to modify the magnet of the SPM in another study. The torque ripple and/or cogging torque can be reduced by modifying the air gap, the stator and rotor core [1-3]. The torque ripple occurs as a result of the energy change along the air gap. Because the reluctance varies along the air gap in a SPM machine [22]. If the tooth geometry is modified by drilling hole(s) into the stator tooth, improvement in the torque ripple will be achieved in this study. Redesigning the stator geometry with drilled teeth to reduce the waviness of the torque reveals the novelty of the work. The examination will be done by creating finite element (FE) model of the OR-SPM machine.

II. Machine Type and Main Parameters

There are two main types of PM machine according to location of the permanent magnet. The magnet of the SPM machine is attached on the surface of the rotor, whereas those of the interior permanent magnet (IPM) machine are buried inside.

In this study, surface-mounted PM machine is selected compared to other PM machines due to the simple structure and low cost. Moreover, the rotor structure of SPM machine has been designed as the outside due to the above reasons. Respectively, the geometry of OR-SPM machine and its the dimensions and performance values are shown in Fig. 1 and Table I.

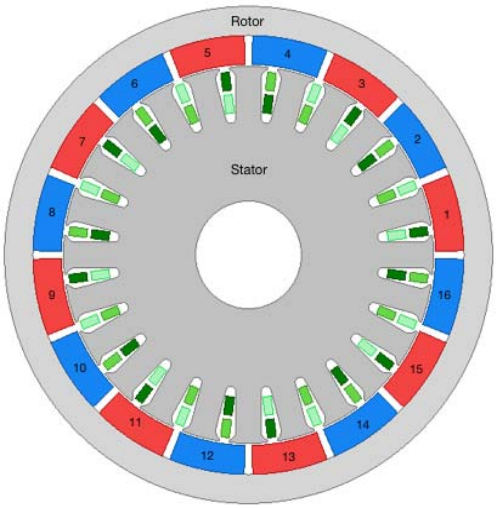

Figure 1. The Outer Rotor SPM Machine with 24s-16p

TABLE I. REFERENCE PARAMETERS OF OR-SPM MACHINE

Parameter	**Value**
Inner & Outer Diameter of Rotor	92-120 mm
Inner & Outer Diameter of Stator	26-91 mm
Height of Rotor & Stator (h_r, h_s)	32.5-14 mm
Stack Length	65 mm
Embrace of Magnet (E_m)	0.9
Offset of Magnet (O_m)	0 mm
Thickness of Magnet (T_m)	7 mm
Slot Opening Height & Width (h_{s0}, b_{s0})	0.5-2.5 mm
Slot Body Height & Bottom Width	9.48-2.5 mm
Slot Wedge Width	5 mm
Slot and Pole Number	24s-16p
Rated Output Power	0.55 kW
Rated Voltage	220 V
Rated speed	1500 rpm
Material of Steel	M19-24G
Material of Magnet	XG196/96

III. Torque Production of PMSM

Torque production in a PMSM is due to the mutual coupling between a permanent magnet and an exciting stator coil. For the magnetic circuit of PMSM, the coenergy stored in the magnetic field written as

$$W_c = \frac{1}{2}Li^2 + \frac{1}{2}\left(R + R_m\right)\phi_m^2 + Ni\phi_m \tag{1}$$

where L inductance of the coil, R and R_m are the reluctances due to excited coil and the magnet, respectively, ϕ_m is the magnet flux linking the coil and N is number of turn of coil.

The change of coenergy according to the rotor angle gives the machine's torque characteristic. As shown below, the torque can be derived by differentiating the coenergy with respect to rotor angle

$$T = \left.\frac{\partial W_c}{\partial \theta}\right|_{i=\text{constant}} \tag{2}$$

By substituting (1) into (2), the torque can be calculated

as

$$T = \frac{1}{2} i^2 \frac{dL}{d\theta} - \frac{1}{2} \phi^2 \frac{dR}{d\theta} + Ni \frac{d\phi}{d\theta} \quad (3)$$

The both of the first two terms in (3) are the reluctance torque associated with the coil and magnet respectively. The first term always acts to increase inductance or permeance and acts to decrease reluctance. The second term is proportional to the square of the magnet flux and the minus sign is that inductance is inversely proportional to reluctance. Furthermore, the second term is called as cogging torque that appears whenever magnet flux travels through a varying reluctance.

$$T_{cog} = -\frac{1}{2} \phi_g^2 \frac{dR_t}{d\theta} \quad (4)$$

where ϕ_g is the magnet flux crossing the air gap and R_t is the total reluctance.

The cogging torque due to the reluctance with respect to rotor angle and also first component of the torque in (3) due to the inductance with respect to rotor angle cause undesired torque ripple. It is actually composed of reluctance of the magnetic circuit generated by the excited winding. Regardless of the magnetic field created by the magnet or coil, changing the reluctance, torque ripple is intended to resolve. If appropriate reluctance change in the magnetic circuit can be achieved, it will be possible to reduce torque ripple.

The cogging torque is also computed at each rotor position using the Maxwell stress tensor on the surface of the rotor.

$$T_{cog} = \frac{l_{stk}}{g \cdot \mu_0} \int_S r_g B_n B_t \cdot dS \quad (5)$$

where is g the air-gap thickness, l_{stk} is the rotor length, r_g is the radius of the air-gap center, B_n and B_t are the air-gap normal and tangential flux densities, respectively. The product of the tangential and normal components of the magnetic flux density are named as T_{factor}

$$T_{factor} = B_n \cdot B_t \quad (6)$$

Torque factor determines the torque characteristic therefore it will be used in through examination.

IV. Finite Element Simulation and Reference Performance Parameters

All analyzes were performed by creating a two-dimensional finite element model of the OR-SPM. After the simulation, important torque values and the THD of back EMF are given in the Table II.

TABLE II. REFERENCE TORQUE PERFORMANCE AND THD OF BACK EMF VALUES FOR RD

Model	T_{avg} (Nm)	T_{rip} (%)	T_{cpp} (Nm)	THD (%)
RD	12.50	5.17	7.71	1.63

These values will be taken as the reference performance values. And OR-SPM machine that has values within the Table I will be referred to as reference design (RD). Performance values that will be available later are compared with the values in Table II.

The torque quantities are the average torque (T_{avg}), the torque ripple (T_{rip}) and the peak-to-peak cogging torque (T_{cpp}). The ripple factor for torque quantity is calculated in the following equations,

$$T_{rip} = \frac{T_{rms}}{T_{avg}} \times 100\% \quad (7)$$

where T_{rms} and T_{avg} respectively the root mean square and the average value of the instantaneous torque. The cogging torque is calculated as a function of the rotor angle under a no-load condition. In that case, only the permanent magnets are in operation for this type of simulation and the stator winding excitation is not in operation.

It was investigated improvement in torque behavior by varying the geometry of slot tooth. The average value of the torque of OR-SPM machine is expected to be large and the torque ripple is expected to be small. Thus, it is aimed to increase the average torque and reduce the torque ripple. Low torque ripple and high average torque are aimed to ensure the boundary condition with B_{limit}<1.8 that is the knee value of BH curve of steel.

V. The Effect of the Slot and Tooth's on Energy Change

The distribution of magnetic flux density [1-3,6-7,21] and the variation in magnetic energy [13-14,16-19] is used to reveal the formation of torque ripple or the cogging torque. In order to understand the behavior of torque in OR-SPM machine in this study, the energy variation that is stored in the magnetic field along the air gap of the machine should be examined. Moreover, it would be useful to establish relationships between these energy changes with the geometry of the machine. A 45-degree cross-sectional view of the OR-SPM is given Fig. 2.

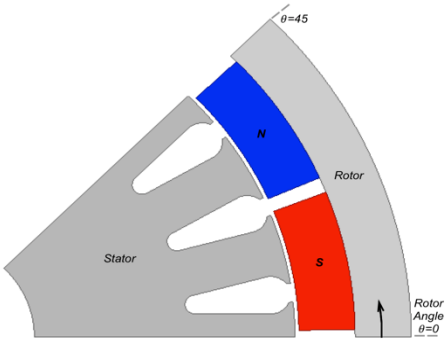

Figure 2. The Cross-Sectional View of The OR-SPM Machine with RD

In Fig. 2, it is necessary to pay attention to where the start (the bottom) and end (the top) of the rotor angle. Because the related curves vary according to the rotor angle are given in accordance with these positions. The rotor also rotates counter-clockwise.

The relationship between variation in the coenergy and the position of the magnet on the rotor is shown in Fig. 3. In addition, the relationship between the T_{factor} and the magnet position is shown in Fig. 4. Since the permanent magnets on the rotor rotate counter-clockwise in Fig. 2, the magnet is placed to move from right to left in Fig. 3 and Fig 4.

As shown in Fig. 3, a significant amount of energy change is made in case the magnet is closer to the slot and is moving away from the slot. It is usually due to high variation in reluctance during the rotation of the rotor.

Therefore, the moment that is dependent on variation in the energy is affected significantly in the slot opening and the tooth shoe region. Thus, it consists of the torque ripple.

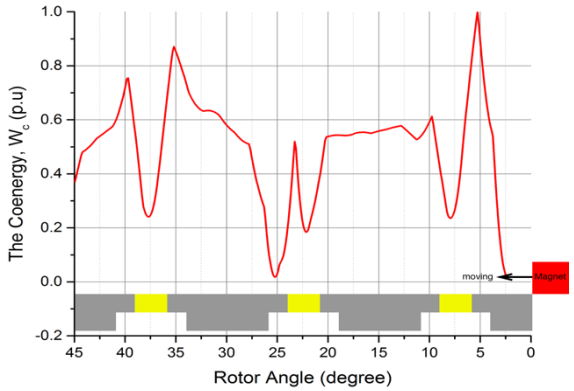

Figure 3. Variation in Coenergy Along Air Gap on the Slot-Tooth Geometry

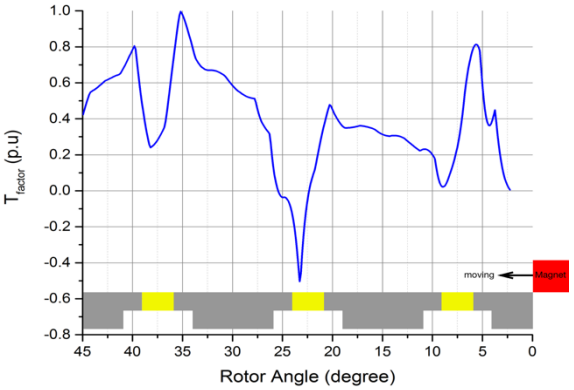

Figure 4. Variation in The Torque Factor Along Air Gap on the Slot-Tooth Geometry

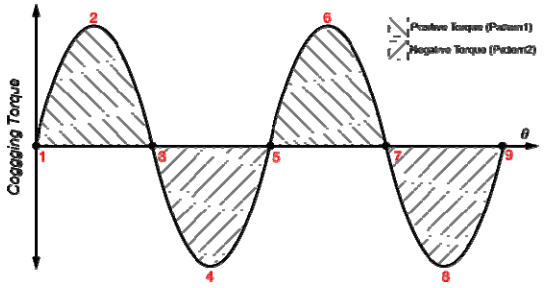

Figure 5. The Cogging Torque with Pattern 1 (P1) and Pattern 2 (P2)

There are special magnet positions according to a slot-tooth pair, when the cogging torque is taken into account (Fig. 5). These special positions of the magnet are numbered in the range 1-9. Four specific magnet positions are shown in Fig 6 and 7. These magnet positions are a magnet is aligned with a slot (MaS), a magnet is aligned with a tooth (MaT), a pair of N-S magnets is unaligned with a slot (MuS) and a pair of N-S magnets is unaligned with a tooth (MuT).

The positive and negative torques in Fig. 5 corresponds to patterned region 1 and 2 in Fig. 6 and 7, respectively. In position 1 and 5, S magnet is in the MaS position and the N magnet is in the MaT position (Fig. 6 and 7). The magnet in MaT position reaches the middle of tooth and the magnet in MaT position reaches the slot opening (position 3 and 7) through the patterned region 1. Meanwhile, the cogging torque takes the maximum value and then becomes zero (position 3 and 7).

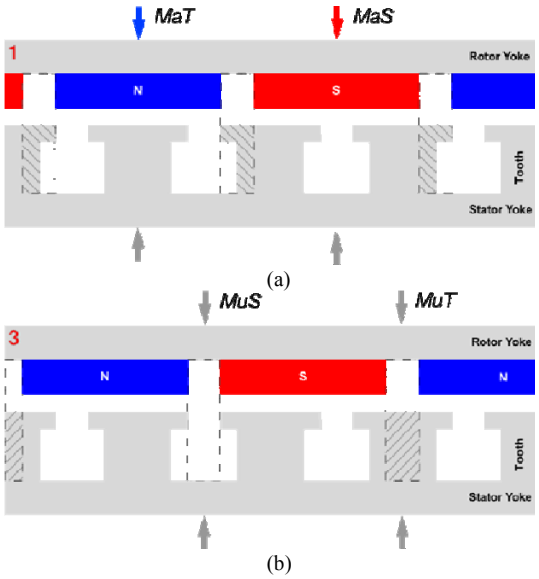

Figure 6. The Magnet Position 1 with P1 (a) and 3 with P2 (b) for First Period of The Cogging Torque

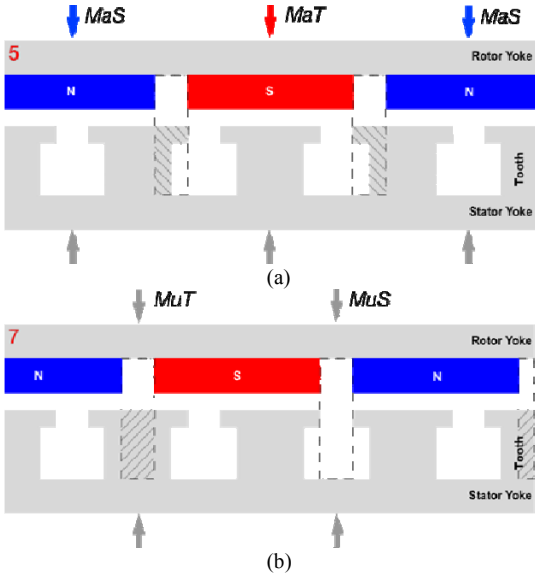

Figure 7. The Magnet Position 5 with P1 (a) and 7 with P2 (b) for Second Period of the Cogging Torque

In position 3 and 7, N and S magnets are in the MuS and MuT positions (Fig. 6 and 7). The magnet in MuT position passes through the patterned region 1 (the tooth) and the magnet in MuS position passes through the patterned region 2 (the slot) (position 5 and 9). Meanwhile, the cogging torque takes the minimum value and then becomes zero (position 5 and 9).

In this examination, the tooth geometry that especially corresponds to the patterned region 1 and 2 will be initially replaced. Thus, the reluctance of the magnetic circuit and fluctuations in the coenergy will be changed.

VI. New Tooth Design For Reducing Torque Ripple

The notch is used to modify uneven distribution flux density of air gap in the IPMSM. Thus, the cogging torque is decreased by notch on the rotor [1]. The notch that has turned into the hole is used in the rotor core in the IPMSM. The torque ripple is reduced by changing tangential components of force density [3]. The modification of the rotor surface shape is considered to reduce the harmonics of

air gap magnetic flux in the IPMSM. Thus, the torque ripple and harmonic components in EMF are decreased by avoiding a rectangular form of air gap flux distribution [2]. The hole in rotor tooth of the SPM machine is considered to modify the variation in magnetic energy in this study.

A new hole is described in the tooth in order to reduce the reluctance of special magnet positions. The hole is shown with its parameters in the center of tooth in Fig. 8. These parameters are as follows away from the center of machine, i.e., the hole height, (h_h), the hole radius (r_h), the angle with the middle tooth i.e., the hole angle (th_h).

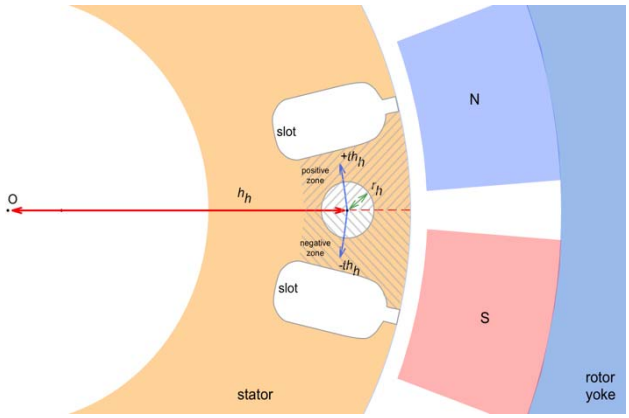

Figure 8. The Described Hole Geometry and Parameters for reducing reluctance

While maintaining the presence of the first hole parameters, the most appropriate location and size of the second hole were investigated to provide the smallest torque ripple. One of the possible hole locations would be in the tooth shoe that is in the patterned region 1. The other location would be on the middle tooth that is in the patterned region 2.

The defined hole is moved in the magnet to determine its location. One third of the length of tooth ($40 \leq h_h \leq 45.5$) is used. In addition, the width of the tooth is divided into positive zone (PZ) that has a positive ($0 \leq th_h \leq 6$) and negative zone (NZ) that has a negative ($0 \geq th_h \geq -6$) hole angle.

The variations in average torque and the torque ripple for the positive zone shown in Fig. 9 and 10, respectively. Similarly, Fig. 11 and 12 show the variations in the average torque and the torque ripple for the negative zone.

In order to easily understand the results of analysis, they are given with half tooth geometry. Shapes with dashed line in the Fig. 9-12 correspond to the left half of the tooth and the right half of the tooth. Important issue is that the torque ripple could not be obtained within the desired limits in the negative zone (Fig. 11 and 12).

When the hole is in the tooth shoe in the positive zone (Fig. 9 and 10), the torque ripple is the smallest value and the average torque is the largest value. After determining the best location of the hole (in P1), the radius of the hole is specified by additional examination as shown in Fig. 13. It is determined as optimum hole radius value, r_h=0.25mm.

In that case, OR-SPM machine will be named as the optimal design 1 (OD1). The geometry of teeth and the detailed torque parameters for OD1 are given Fig. 14 and Table III, respectively. Obtained variation values in Table III are calculated according to Table II.

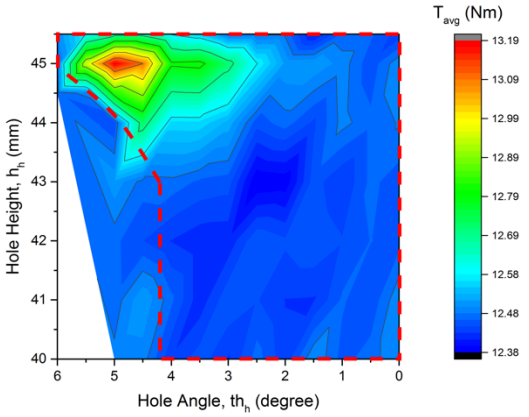

Figure 9. The Average Torque Variation in Positive Zone

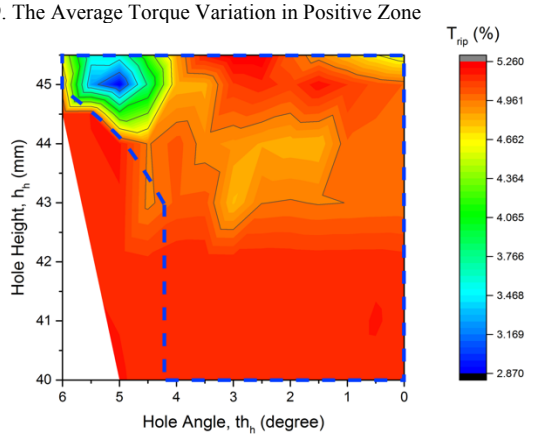

Figure 10. The Torque Ripple Variation in Positive Zone

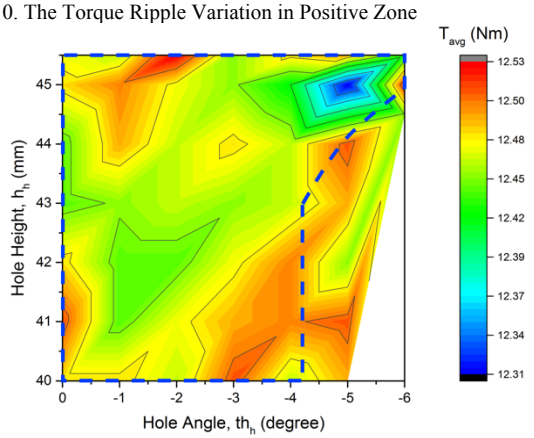

Figure 11. The Average Torque Variation in Negative Zone

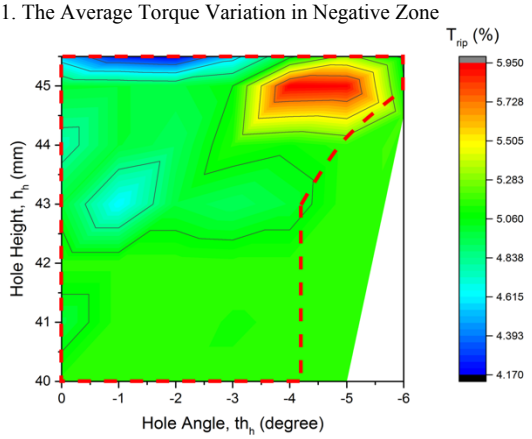

Figure 12. The Torque Ripple Variation in Negative Zone

As can be seen from Table III, it was achieved 44.5% reduction in the torque ripple and small increment in the average torque (5.9%). The THD is reduced by 14%. However, the cogging torque value has increased slightly rather than decreased.

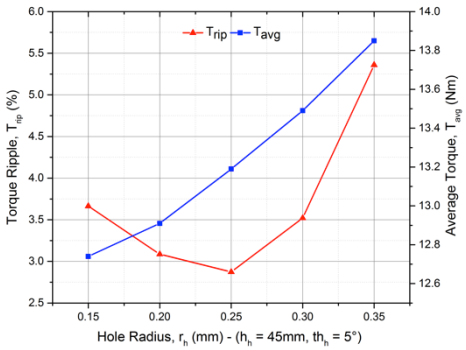

Figure 13. The Variation in the First Hole Radius

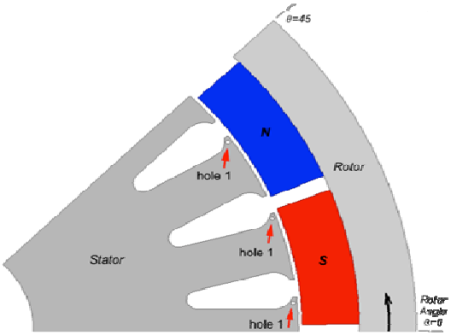

Figure 14. The Hole Location in P1 for OR-SPM Machine with OD1

TABLE III. THE TORQUE PARAMETERS FOR OD1

T_{avg} (Nm)	ΔT_{avg} (%)	T_{rip} (%)	ΔT_{rip} (%)	T_{cpp} (Nm)	ΔT_{cpp} (%)	THD (%)	ΔTHD (%)
13.19	5.9%	2.87	-44.5%	7.96	3.2%	1.40	-14.1%
h_h = 45 mm, th_h = 5°, r_h = 0.2 mm (OD1)							

The variation curve of the coenergy and the torque factor is given in Fig. 15 and 16, respectively. These will be used to explain the decline in the torque ripple.

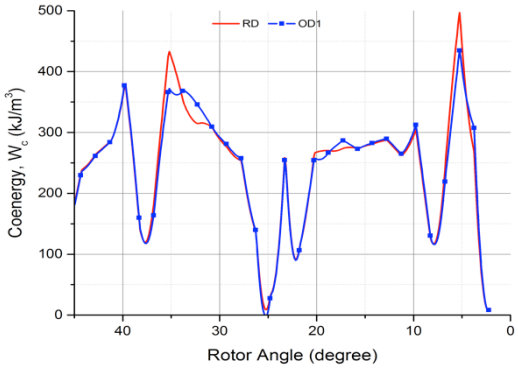

Figure 15. The Coenergy Variation for RD and OD1

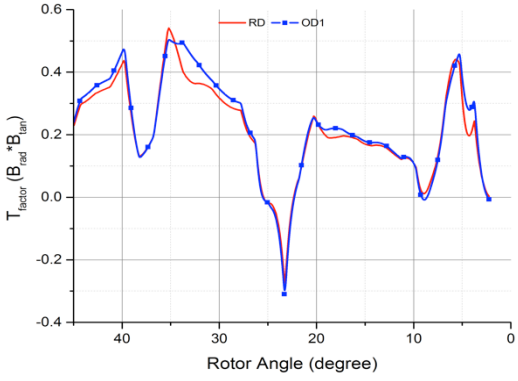

Figure 16. The Torque Factor Variation for RD and OD1

Although the cogging torque that is generated by the zero coil current has not decreased, reduction in the peaks of the coenergy and the torque factor is realized according to these figures. OR-SPM machine with OD1 has low fluctuation compared to reference design (RD).

VII. IMPROVING TOOTH DESIGN WITH ADDITIONAL HOLE

Definition a hole in the tooth shoe has given satisfactory results with respect to reference design (RD). A second hole that is described in the patterned region 1 and 2 will still create similar positive effects. New hole parameters that are named subscript 2 will be valid for the second hole. These second parameters are as follows; the second hole height (h_{h2}), the second hole radius (r_{h2}), the second hole angle, (th_{h2}). The parameter values of the first hole are kept constant during second examination. The variations in the average torque and the torque ripple for the positive and negative zone are shown in Fig. 17-20.

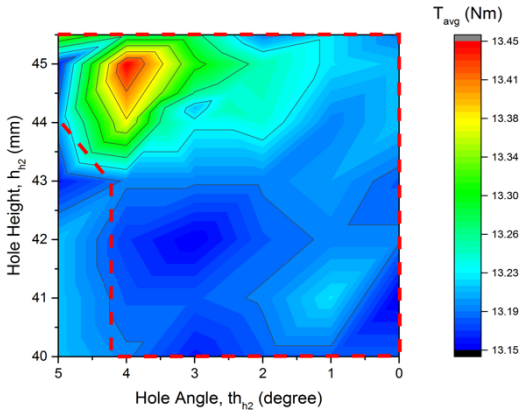

Figure 17. The Average Torque Variation in Positive Zone

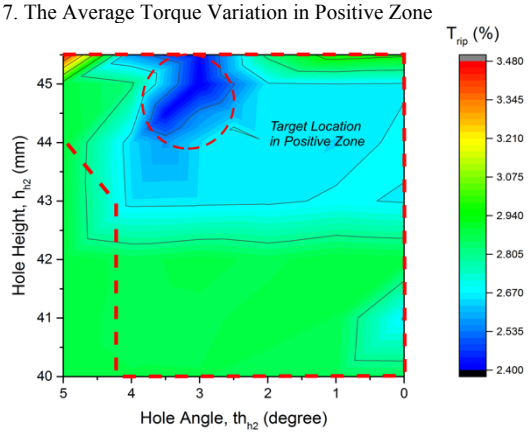

Figure 18. The Torque Ripple Variation in Positive Zone

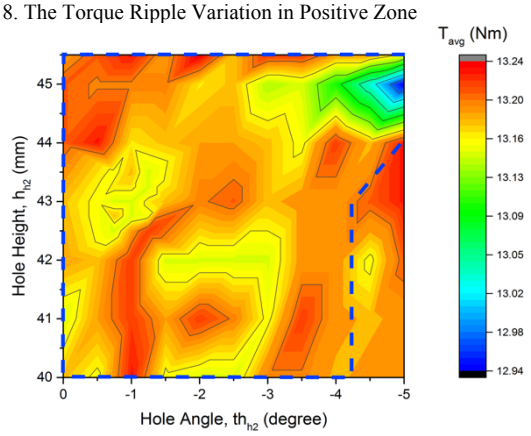

Figure 19. The Average Torque Variation in Negative Zone

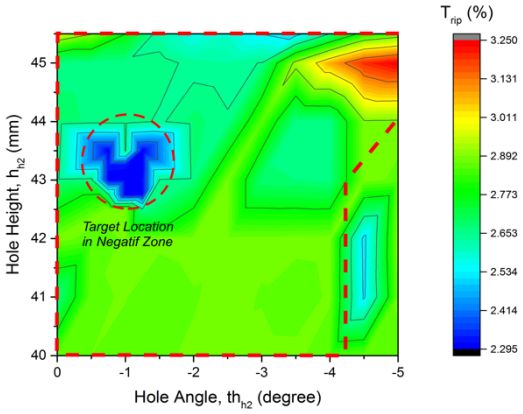

Figure 20. The Torque Ripple Variation in Negative Zone

In Fig. 18 and 20, two target locations (in P1 and P2) where the torque ripple is quite low were observed. It should be noted that these locations correspond to the patterned region 1 and 2 (in Fig. 6 and 7). Thus, the hole parameters that are selected from Fig. 18 and 20 according to best torque value are given in Table IV.

TABLE IV. THE SECOND HOLE AND TORQUE PARAMETERS

$th_h = 5^\circ$, h_h = 45mm, r_h = 0.25mm (OD1)					
Location -	**h_{h2}** (mm)	**th_{h2}** ($^\circ$)	**r_{h2}** (mm)	**T_{avg}** (Nm)	**T_{rip}** (%)
NZ	43	-1	0.2	13.15	2.30
PZ	45	3	0.2	13.31	2.40

After determining the two best location of the hole (in P1 and P2), the radii of holes were specified by additional examination. Thus, optimum radius values of the two holes were determined as 0.25mm and 0.2mm according to Fig. 21 and 22.

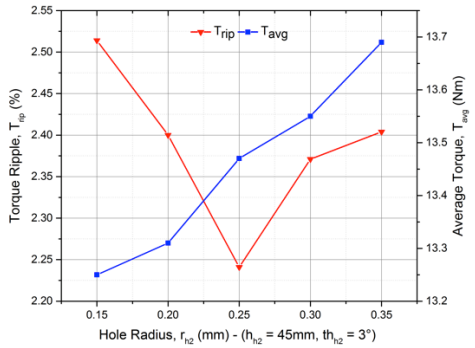

Figure 21. The Torque Ripple and the Average Torque Variation in the Hole Radius in Positive Zone

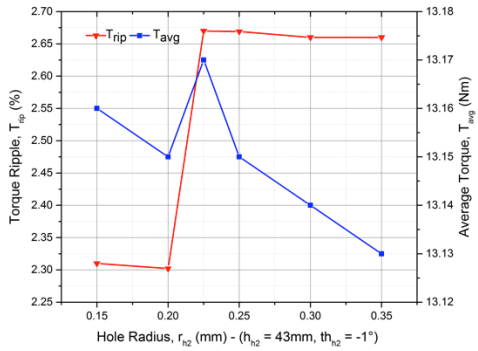

Figure 22. The Torque Ripple and the Average Torque Variation in the Hole Radius in Negative Zone

If the second hole is used in the positive zone, optimum design 2 (OD2) is obtained. Likewise, the optimum design 3 (OD3) is obtained for negative zone.

The detailed torque parameters are given in the Table V. As seen from the Table V, the torque ripples of the two OR-SPM models (OD2 and OD3) are very similar. However, the OD3 model appears to be more advantageous in terms of the THD of back EMF (-12.3%), and the OD1 model is more advantageous in terms of the average torque (8.2%)

There are 5.5% and 8.2% improvement in the average torque. The torque ripple value is provided by 56.7% and 55.3% improvement. Particularly, the improvement in the value of the torque ripple is quite successful.

TABLE V. THE TORQUE PARAMETERS FOR OD2 AND OD3

$th_h = 5^\circ$, h_h = 45mm, r_h = 0.25mm (OD1)							
T_{avg} (Nm)	**ΔT_{avg}** (%)	**T_{rip}** (%)	**ΔT_{rip}** (%)	**T_{cpp}** (Nm)	**ΔT_{cpp}** (%)	**THD** (%)	**ΔTHD** (%)
13.47	8.2%	2.24	-56.7%	7.67	-0.5%	1.52	-6.7%
h_{h2} = 45 mm, th_{h2} = 3°, r_{h2} = 0.25 mm (OD2 in P1)							
13.13	5.5%	2.31	-55.3%	7.75	0.5%	1.43	-12.3%
h_{h2} = 43 mm, th_{h2} = -1°, r_{h2} = 0.2 mm (OD3 in P2)							

The cross-sectional view of the OR-SPM with OD2 and OD3 are given in the Fig. 23. It is necessary to note that there are two holes in both models. The first hole corresponds to OD1 (Fig. 14). The second hole is specific to OD2 or OD3. Shapes with dashed line in the Fig. 23 correspond to the patterned region 1 (P1) and 2 (P2) in the Fig. 6 and 7. It was predicted that holes that are described in the patterned region 1 and 2 would reduce the torque ripple.

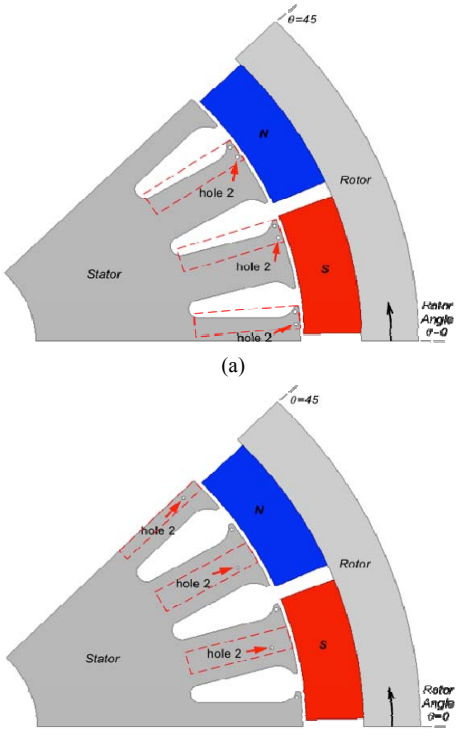

Figure 23. The Hole Location in P1 for OR-SPM machine with OD2 (a) The Hole Location in P2 for OR-SPM machine with OD3 (b)

One of the two holes is located in the patterned region 1 and the other is in the patterned region 2 for the OR-SPM with OD3, whereas both two holes is located in the patterned region 1 for the OR-SPM with OD3.

As seen in Fig. 15, fluctuation in coenergy is decreasing due to model OD1. This variation is likewise given in Fig. 24 for OD2 and OD3. It is observed that the energy variation still continuing. Similarly, fluctuation is also reduced due to OD2 and OD3. Although calculated cogging torque that is generated by the zero coil current is unchanged, the energy variation in the curve illustrates the reduction of the torque ripple (Fig. 24).

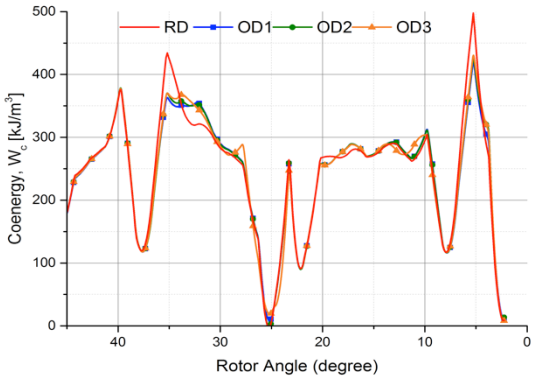

Figure 24. The Coenergy Variation for RD, OD1, OD2 and OD3

VIII. Conclusion

The stator tooth geometry that especially corresponds to the patterned region 1 and 2 will be an important function of the magnetic energy variation along with air gap. Thus, the reluctance of the magnetic circuit and fluctuations in the magnetic energy will be changed by drilling a hole into the stator tooth. Firstly, the effect of a hole on the magnetic energy variation and torque ripple is investigated. It was achieved 44.5% reduction in the torque ripple with model that is named as OD1. Subsequently, improvements provided by the second hole were investigated. 56.7% and 55.3% improvement in the torque ripple value of models that are named as OD2 and OD3 was achieved, respectively. Additionally, there has been improvement in the average torque value and THD of back EMF with the new stator tooth geometry.

References

[1] S.-H. Lee, K.-K. Han, H.-J. Ahn, G.-H. Kang, Y.-D. Son and G.-T. Kim,"A Study on Reduction of Vibration Based on Decreased Cogging Torque for Interior Type Permanent Magnet Motor", in IEEE Industry Applications Society Annual Meeting (IAS'08), Edmonton, Alta, Canada, 2008, pp. 1-6. doi: 10.1109/08IAS.2008.40

[2] S. Un-Jae, C. Yon-Do, C. Jae-Hak, H. Pil-Wan, K. Dae-Hyun and L. Ju, "A Technique of Torque Ripple Reduction in Interior Permanent Magnet Synchronous Motor", IEEE Transactions on Magnetics, vol. 47, no. 10, pp. 3240-3243, 2011. doi: 10.1109/TMAG.2011.2150742

[3] S.-K. Lee, G.-H. Kang, J. Hur and B.-W. Kim, "Stator and Rotor Shape Designs of Interior Permanent Magnet Type Brushless DC Motor for Reducing Torque Fluctuation", IEEE Transactions on Magnetics, vol. 48, no. 11, pp. 4662-4665, 2012. doi: 10.1109/TMAG.2012.2201455

[4] T. Ishikawa and G. R. Slemon, "A Method of Reducing Ripple Torque in Permanent Magnet Motors Without Skewing", IEEE Transactions on Magnetics, vol. 29, no. 2, pp. 2028-2031, 1993. doi: 10.1109/20.250808

[5] R. Lateb, N. Takorabet and F. Meibody-Tabar, "Effect of Magnet Segmentation on the Cogging Torque in Surface-Mounted Permanent-Magnet Motors", IEEE Transactions on Magnetics, vol. 42, no. 3, pp. 442-445, 2006. doi: 10.1109/TMAG.2005.862756

[6] Y. Yang, X. Wang, C. Zhu and C. Huang,"Study of Magnet Asymmetry for Reduction of Cogging Torque in Permanent Magnet Motors", in 4th IEEE Conference on Industrial Electronics and Applications, Xi'an, China, 2009, pp. 2325-2328. doi: 10.1109/ICIEA.2009.5138614

[7] R. Islam, I. Husain, A. Fardoun and K. McLaughlin, "Permanent-Magnet Synchronous Motor Magnet Designs With Skewing for Torque Ripple and Cogging Torque Reduction", IEEE Transactions on Industry Applications, vol. 45, no. 1, pp. 152-160, 2009. doi: 10.1109/TIA.2008.2009653

[8] J. Seok-Myeong, P. Hyung-Il, C. Jang-Young, K. Kyoung-Jin and L. Sung-Ho, "Magnet Pole Shape Design of Permanent Magnet Machine for Minimization of Torque Ripple Based on Electromagnetic Field Theory", IEEE Transactions on Magnetics, vol. 47, no. 10, pp. 3586-3589, 2011. doi: 10.1109/TMAG.2011.2151846

[9] W. Q. Chu and Z. Q. Zhu, "Investigation of Torque Ripples in Permanent Magnet Synchronous Machines With Skewing", IEEE Transactions on Magnetics, vol. 49, no. 3, pp. 1211-1220, 2013. doi: 10.1109/TMAG.2012.2225069

[10] P. Upadhyay and K. R. Rajagopal,"Torque Ripple Minimization of Interior Permanent Magnet Brushless DC Motor Using Rotor Pole Shaping", in International Conference on Power Electronics, Drives and Energy Systems (PEDES'06), 2006, pp. 1-3. doi: 10.1109/PEDES.2006.344369

[11] C. C. Hwang, M. H. Wu and S. P. Cheng, "Influence of Pole and Slot Combinations on Cogging Torque in Fractional Slot PM Motors", Journal of Magnetism and Magnetic Materials, vol. 304, no. 1, pp. e430-e432, 2006. doi: 10.1016/j.jmmm.2006.01.207

[12] D. Wu and Z. Q. Zhu, "Design Tradeoff Between Cogging Torque and Torque Ripple in Fractional Slot Surface-Mounted Permanent Magnet Machines", IEEE Transactions on Magnetics, vol. 51, no. 11, pp. 1-4, 2015. doi: 10.1109/TMAG.2015.2436714

[13] B. Ackermann, J. H. H. Janssen, R. Sottek and R. I. Van Steen, "New Technique for Reducing Cogging Torque in a Class of Brushless DC Motors", Electric Power Applications, IEE Proceedings B, vol. 139, no. 4, pp. 315-320, 1992. doi: 10.1049/ip-b.1992.0038

[14] C. Breton, J. Bartolome, J. A. Benito, G. Tassinario, I. Flotats, C. W. Lu and B. J. Chalmers, "Influence of Machine Symmetry on Reduction of Cogging Torque in Permanent-Magnet Brushless Motors", IEEE Transactions on Magnetics, vol. 36, no. 5, pp. 3819-3823, 2000. doi: 10.1109/20.908386

[15] Z. Q. Zhu and D. Howe, "Influence of Design Parameters on Cogging Torque in Permanent Magnet Machines", IEEE Transactions on Energy Conversion, vol. 15, no. 4, pp. 407-412, 2000. doi: 10.1109/60.900501

[16] N. Bianchi and S. Bolognani, "Design Techniques for Reducing the Cogging Torque in Surface-Mounted PM Motors", IEEE Transactions on Industry Applications, vol. 38, no. 5, pp. 1259-1265, 2002. doi: 10.1109/TIA.2002.802989

[17] C. S. Koh and J.-S. Seol, "New Cogging-Torque Reduction Method for Brushless Permanent-Magnet Motors", IEEE Transactions on Magnetics, vol. 39, no. 6, pp. 3503-3506, 2003. doi: 10.1109/TMAG.2003.819473

[18] Y. D. Yao, D. R. Huang, J. C. Wang, S. H. Liou, S. J. Wang, T. F. Ying and D. Y. Chiang, "Simulation Study of The Reduction of Cogging Torque in Permanent Magnet Motors", IEEE Transactions on Magnetics, vol. 33, no. 5, pp. 4095-4097, 1997. doi: 10.1109/20.619674

[19] C. S. Koh, H. S. Yoon, K. W. Nam and H. S. Choi, "Magnetic pole shape optimization of permanent magnet motor for reduction of cogging torque", IEEE Transactions on Magnetics, vol. 33, no. 2, pp. 1822-1827, 1997. doi: 10.1109/20.582633

[20] M. Fazil and K. R. Rajagopal, "A Novel Air-Gap Profile of Single-Phase Permanent-Magnet Brushless DC Motor for Starting Torque Improvement and Cogging Torque Reduction", IEEE Transactions on Magnetics, vol. 46, no. 11, pp. 3928-3932, 2010. doi: 10.1109/TMAG.2010.2057514

[21] I. Petrov, P. Ponomarev, Y. Alexandrova and J. Pyrhonen, "Unequal Teeth Widths for Torque Ripple Reduction in Permanent Magnet Synchronous Machines With Fractional-Slot Non-Overlapping Windings", IEEE Transactions on Magnetics, vol. 51, no. 2, pp. 1-9, 2015. doi: 10.1109/TMAG.2014.2355178

[22] D. C. Hanselman, "Brushless permanent magnet motor design", pp. 45-181, The Writers' Collective, 2003.